

Synthesis, Characterization and Activity of Sulphate-modified V₂O₅/SnO₂ Catalysts

Sreejarani K. Pillai and Omanakutty Gheevarghese*

Department of Chemistry, Tshwane University of Technology, Pretoria 0001, South Africa.

Received 19 July 2007, revised 8 February 2008, accepted 13 February 2008.

ABSTRACT

Sulphate-modified V₂O₅/SnO₂ catalysts were prepared by a simple impregnation method and characterized using different physicochemical techniques, such as EDX, BET-SA, XRD, FT-IR, TGA and ⁵¹V NMR spectroscopy. A simple, effective and environmentally friendly method for the gas phase conversion of cyclohexanone oxime to ε-caprolactam by these modified catalysts is presented. The optimal protocol allows ε-caprolactam to be synthesized in excellent yields. NH₃-TPD and cumene conversion reactions were used to determine the acid structural properties of the catalysts. Definite correlation was observed between the concentration of medium strength acid sites or Brønsted sites and the ε-caprolactam selectivity. Time-on-stream studies showed fast decline in the activity of the catalyst resulting from the basic nature of the reactant and product molecules.

KEYWORDS

Sulphated V₂O₅/SnO₂ catalysts, acidity, vapour phase Beckmann rearrangement.

1. Introduction

ε-Caprolactam, an important intermediate for the production of nylon-6 fibres and resins, is industrially produced by the liquid phase Beckmann rearrangement of cyclohexanone oxime using highly concentrated sulphuric acid as catalyst.¹ Despite its high selectivity, this homogeneous catalyst offers several disadvantages, like the production of large amounts of undesirable ammonium sulphate, corrosion and environmental problems. In the constant search for cleaner technologies, there is a definite need for the use of the catalytic Beckmann rearrangement, especially in the vapour phase over solid acid catalysts.² A number of solid catalysts have been studied in the vapour phase Beckmann rearrangement of cyclohexanone oxime, including silica-alumina,³ tantalum oxides,⁴ molecular sieves^{5–9} and zeolites.^{10–12}

Previous researchers have highlighted the use of single-component oxides in the vapour phase Beckmann rearrangement, such as alumina, silica, thoria, titania and zirconia, as well as B₂O₃-based catalysts.¹³ Recently Mao *et al.* reported B₂O₃/TiO₂-ZrO₂ as an effective catalyst compared with other B₂O₃-supported pure metal oxides.^{14–16} Guo *et al.*¹⁷ have demonstrated silica-pillared layered niobic acid as an efficient catalyst for the reaction in the presence of 1-hexanol. Compared with the conventional method, solid acid catalysis is an environmentally benign route since there is no undesirable formation of ammonium sulphate.¹⁸

Vanadia-supported metal oxide catalysts are the basic components of several industrial catalysts, which are used for the selective oxidation and ammoxidation of various hydrocarbons and for the selective catalytic reduction of NO_x with NH₃.^{19–23} Furthermore, it has been well documented that the selectivity and activity of these supported vanadia catalysts for various reactions depend on the acid–base properties of the support, calcination temperature and the percentage of vanadia loading. Thus, careful choice of the support, suitable preparation procedure and precise amount of vanadia loading are found to be the crucial factors in the preparation of vanadia catalysts for a specific reaction.^{24,25}

SnO₂, much like TiO₂, Fe₂O₃, UO₃, etc., is a metal oxide included in Group B, which is intermediate between the acidic metal oxides like V₂O₅, MoO₃ and WO₃ (Group A) and basic metal oxides such as NiO, MnO₂, CuO and Cr₂O₃ (Group C).²⁶ It is reported that the acid–base properties of the SnO₂ systems vary significantly by the introduction of a small quantity of acidic or basic elements. Above all, the characteristic features of the selectivity become completely different when different types of metal oxides are incorporated into SnO₂.²⁷ For instance, the catalytic property of SnO₂ in benzene formation is greatly enhanced by the addition of basic oxides, whereas acrolein formation is promoted by acidic oxides.²⁸

In the present paper, we discuss the applicability of sulphate-modified V₂O₅/SnO₂ catalysts as a preferable alternative in vapour phase Beckmann rearrangement. The application of V₂O₅/SnO₂ catalysts for the above reaction has not yet been investigated to the best of our knowledge. To examine the catalytic efficiencies we prepared a series of V₂O₅/SnO₂ catalysts, surface-modified by sulphate groups. These systems were characterized by EDX, BET-SA, XRD, FT-IR, TGA and ⁵¹V NMR techniques. NH₃-TPD (temperature programmed desorption) and hydrocracking of cumene were performed to characterize the acidity of the sulphated catalysts with different V₂O₅ loadings. The catalytic performance of these systems for vapour phase Beckmann rearrangement was investigated under optimized reaction conditions.

2. Experimental

2.1. Catalyst Preparation

SnO₂ was prepared from stannic chloride by the hydroxide method,²⁹ using 1:1 ammonia solution. The wet impregnation of SnO₂ with oxalic acid solution of ammonium metavanadate³⁰ produced catalyst samples with various V₂O₅ contents. The V₂O₅ loading was varied from 3 to 15 mass %, as indicated by the number in the sample notation. The sulphate modification of the samples (single and supported oxides) was done with 0.5 mol L⁻¹

* To whom correspondence should be addressed: E-mail: gheevargheseo@tut.ac.za

Table 1 Surface properties of sulphated V₂O₅/SnO₂ catalysts.

System	BET surface area/m ² g ⁻¹	Pore volume/cm ³ g ⁻¹	Elemental composition by EDX/%		
			Sn	V	S
T0	25	0.023	78.8	–	–
ST0	79	0.081	77.9	–	0.3
ST3	87	0.086	–	–	0.5
ST6	95	0.096	73.3	3.7	0.6
ST9	118	0.110	69.9	5.7	0.9
ST12	89	0.092	–	–	–
ST15	74	0.072	–	–	–

H₂SO₄ (5 mL g⁻¹). The precipitate was filtered without washing, dried at 383 K overnight, sieved below 100 μm and calcined at 823 K for 5 h. The general sample notation STX stands for sulphated SnO₂ with X mass % of V₂O₅, whereas T0 denotes pure SnO₂.

2.2. Catalyst Characterization

Simultaneous determination of BET surface area and total pore volume of the samples was achieved in a Micromeritics Gemini surface area analyser by the N₂ adsorption technique at liquid nitrogen temperature. The elemental compositions of the sulphate-doped samples were determined using EDX analysis in a Stereoscan 440 apparatus (two measurements per data point). The crystal structures of the samples were identified by XRD (Rigaku D-max C X-ray diffractometer) measurement using Ni-filtered CuK_α radiation (λ = 1.5406 Å). FTIR spectra of the powder samples were measured by the KBr disc method over the range 4000–400 cm⁻¹ using a Shimadzu DR 5001 instrument. A Shimadzu TGA-50 instrument was used for carrying out thermogravimetric studies. About 20 mg of the sample was used at a heating rate of 20 K min⁻¹ in N₂ atmosphere. ⁵¹V NMR spectra of the prepared samples were recorded using a Bruker 300 DSX instrument with a static magnetic field of 8.5 T. The spectra were recorded with a reference signal of NH₄VO₃ at a chemical shift value of 0 ppm and higher frequency shifts from the standard were taken as positive.

Ammonia-TPD measurements, performed in the range 373–873 K in a conventional flow-type apparatus at a heating rate of 10 K min⁻¹ with nitrogen atmosphere, were used to estimate the acidic properties of the developed catalysts. 100 mg of the catalyst was placed in a tubular reactor and heated to 473 K under nitrogen flow for approximately 4–5 h. The reactor was then cooled and the adsorption of ammonia was conducted by exposing the sample to ammonia at a flow rate of 10 mL min⁻¹ for 1 h. The acid strength distribution was subsequently determined by raising the temperature in steps, *viz.* 373–473, 473–673 and 673–873 K, with the flow of nitrogen. The cumene conversion reaction was adopted for the differentiation between Brønsted and Lewis acid sites. The reaction was carried out in a continuous down-flow reactor at 623 K at a flow rate of 6 mL h⁻¹ and with a time on stream of 2 h. The product analysis was achieved gas chromatographically (Chemito 8610 GC, SE-30 column, 393 K isothermal, injector and detector temperatures 503 K) by comparison with authentic samples.

2.3. Catalytic Reaction Procedure

The vapour phase Beckmann rearrangement reaction was conducted at atmospheric pressure in a fixed-bed, vertical, down-flow quartz reactor (0.6 cm internal diameter and 30 cm height) inserted into a double-zone furnace. The catalyst in powdered form (0.5 g) was immobilized using glass wool and

sandwiched between inert silica beads. A thermocouple positioned near the catalyst bed monitored the reaction temperature, which was regulated using a high sensitivity temperature controller (accuracy ±5 K). The feed containing cyclohexanone oxime in benzene (diluent) was introduced to the reactor using a syringe pump at a flow rate of 5 mL h⁻¹ at 523 K. The reactor effluents including ε-caprolactam were collected downstream at the end of a water condenser and analysed by a Chemito 8610 GC equipped with SE-30 column and FID detector. The temperature programme used for the column was 363 K, 3 min, 5 K, 513 K, in the sequence initial temperature, duration, rate of increase, and final temperature, respectively, while the injector-detector temperature was 523 K. Among the various products formed, only ε-caprolactam and cyclohexanone were estimated separately, while all the remaining minor products (5-cyanopentane, 5-cyano-pent-1-ene and 2-cyclohexen-1-one) were grouped together as 'others' during the calculation of selectivity. Another set of experiments was carried out to establish the stability of the systems to the deactivation processes. The performance of the reaction for a continuous 5 h run was used to investigate the susceptibility of deactivation of the catalyst. The products were collected and analysed every hour.

3. Results and Discussion

3.1. Physicochemical Characteristics

The BET analysis data (Table 1) show a remarkable enhancement of surface area and pore volume of single oxide after sulphate modification, which may be attributed to the retardation of crystallization due to the sulphate groups present on the surface.³¹ In the vanadia-containing systems, the properties reach a maximum value at 9% V₂O₅ loading and decline thereafter. The dispersed vanadia particles, along with the sulphate species, can prevent the agglomeration of tin oxide particles, leading to an enhanced surface area at low loading.³² At high vanadia loading, the crystalline V₂O₅ formed can block the pores of the tin oxide support, leading to a reduction of the surface area. The repartition of the pore volume at high loading also supports the dramatic plugging of pores with V₂O₅ particles and sulphate groups.³³

The EDX data (Table 1) show that the amount of sulphur in vanadia-promoted samples is considerably higher than in the simple sulphated sample ST0, although the same concentration of sulphuric acid solution was used for sulphate modification of all the samples. The sulphur content increased from 0.3 to 0.9% as the V₂O₅ content was increased from 0 to 9 mass %. This confirms the fact that the presence of vanadia stabilizes the sulphate over layers on the catalyst surface.

The XRD patterns (Fig. 1) show that tin oxide is in a tetragonal active phase in the pure as well as the sulphated forms. The XRD profiles of the sulphated systems show only a trivial broadening of the peaks. It has been reported that the degree of crystalliza-

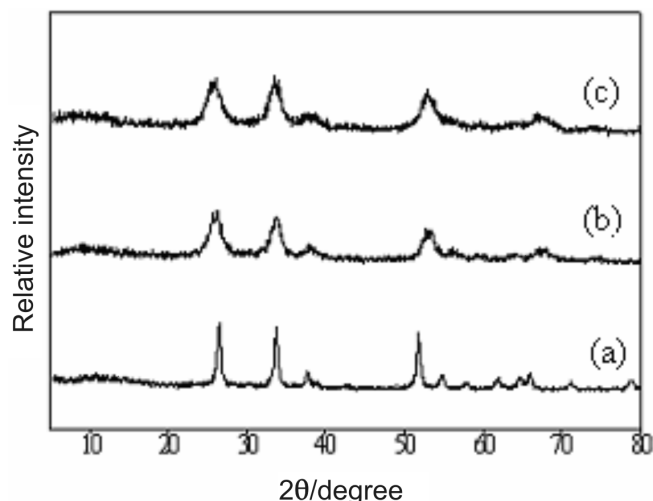


Figure 1 XRD patterns of various SnO_2 samples: (a) T0, pure SnO_2 ; (b) T6, 6% $\text{V}_2\text{O}_5/\text{SnO}_2$; (c) ST6, sulphate-modified T6.

tion of the sulphated oxides is much lower than that of the oxides without sulphate treatment.³⁴ The absence of any change in the peak intensity after sulphate treatment indicates that the amount of sulphate retained on the surface is insufficient to cause any change in the diffraction pattern and that it is well dispersed on the surface without entering into the bulk of the catalyst.

The IR spectrum of pure tin oxide contains three major absorption bands at 3424, 1642 and 619 cm^{-1} (Fig. 2). The first two bands may be attributed to the hydroxyl groups associated with the structural water³⁵ and the third to the Sn-O bonds of the support.³⁶ The IR spectra of all the sulphated samples show absorption bands at 1210, 1150–1130, 1070–1060 and 980–960 cm^{-1} , apart from the bands present at 2046, 1030 and 845 cm^{-1} . The former group of bands is consistent with the bidentate complex structure of the sulphate ligand, while the latter set corresponds to the V=O stretching mode and its first overtone. The peaks in the 1200–1100 cm^{-1} range can be assigned to the S=O group.^{37,38} The bands around 3420 and 1640 cm^{-1} correspond to the stretching and bending modes of –OH groups present in the catalysts.

The TG-DTG curve of pure SnO_2 shows a dip near 373 K, due to

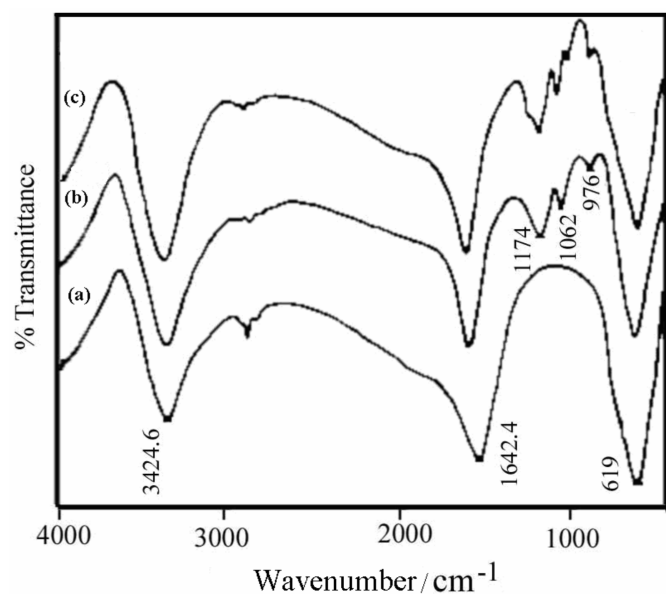


Figure 2 FT-IR spectra of various SnO_2 samples (a) T0, pure SnO_2 ; (b) ST0, sulphated SnO_2 ; (c) ST6, sulphate-modified V_2O_5 (6%)/ SnO_2 .

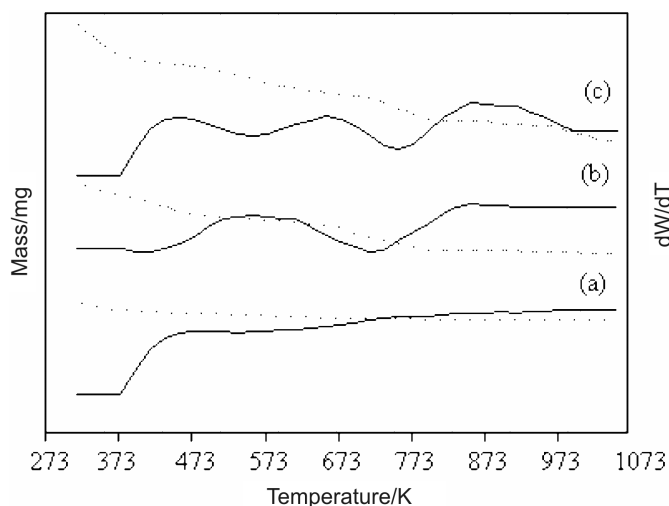


Figure 3 TG-DTG curves of various samples: (a) T0, pure SnO_2 ; (b) T6, V_2O_5 (6%)/ SnO_2 ; (c) ST6 – sulphate-modified T6.

the removal of physisorbed water from the catalyst surface (Fig. 3). In the case of the sulphated vanadia-promoted sample ST6, additional mass losses at about 453 K, 723 K and 973 K are also observed. The first two mass losses are due to NH_4VO_3 decomposition with the release of two molecules of NH_3 and one of H_2O , giving rise to an intermediate $(\text{NH}_4)_2\text{O}(\text{V}_2\text{O}_5)_3$, which eventually transforms to V_2O_5 .³⁹ The third one reveals the commencement of decomposition of sulphate into SO_2/SO_3 vapour above 973 K.⁴⁰

⁵¹V NMR spectra of the $\text{V}_2\text{O}_5/\text{SnO}_2$ catalysts show two types of major signals, a shoulder at δ 257.9 ppm and an intense peak at δ 150.3 ppm (Fig. 4). The NMR spectra of the sulphated sample ST6 is very similar to that of its unmodified counterpart, T6. A low value for the chemical shift in the wide-line NMR spectrum is characteristic of vanadium oxide in low coordination (tetrahedral), while a higher value is assigned to a higher (octahedral) coordination, based on the spectra of various known vanadium oxide-containing compounds.^{41–43}

3.2. Catalyst Acidity Measurement

NH_3 -TPD enables the characterization of the acid strength distribution of the solid acid catalyst systems. This procedure is

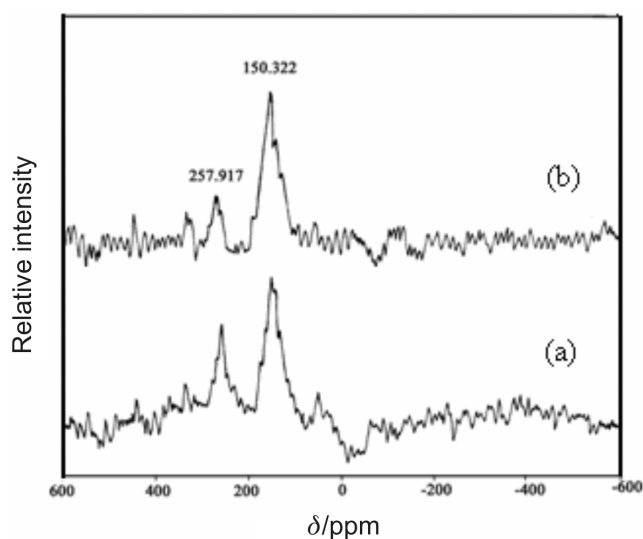


Figure 4 ⁵¹V NMR spectra of (a) T6 V_2O_5 (6%)/ SnO_2 ; (b) ST6, sulphate-modified T6.

Table 2 Acidic properties and catalytic activities of various sulphated V₂O₅/SnO₂ catalysts.

Catalyst	Amount of ammonia desorbed from NH ₃ -TPD/mmol g ⁻¹			Hydrocracking of cumene ^a	Vapour phase Beckmann rearrangement ^b	
	Weak, 373–473 K	Medium, 473–673 K	Strong, 673–873 K	Cracking product selectivity/%	Conversion/mass %	ϵ -Caprolactam selectivity/%
T0	0.32	0.36	0.12	10.0	29.5	16.8
ST0	0.55	0.45	0.25	17.5	59.3	25.5
ST3	0.56	0.54	0.29	23.6	94.7	42.2
ST6	0.63	0.61	0.31	28.9	98.4	58.7
ST9	0.59	0.69	0.26	34.7	100	71.2
ST12	0.54	0.63	0.18	26.8	96.7	56.5
ST15	0.43	0.56	0.15	14.5	90.7	22.1

^a Mass of catalyst 0.5 g, temperature 623 K, flow rate 6 mL h⁻¹, time on stream 2 h.

^b Mass of catalyst 0.5 g, temperature 523 K, flow rate 5 mL h⁻¹, time on stream 2 h.

considered as a standardization method since ammonia allows the determination of both the protonic and cationic acidities by titrating acid sites of any strength. A fairly reliable interpretation of the TPD pattern of ammonia from solid acids can be attributed to ammonia chemisorbed on weak (desorption in the temperature range 373–473 K), medium (473–673 K) and strong (673–873 K) sites respectively, although it is not yet possible to discriminate between Brønsted and Lewis acidic sites.^{44,45}

Vapour phase cumene cracking is a model reaction in identifying the Lewis/Brønsted acidity of a catalyst. The major reactions occurring during cumene conversion may be grouped into dealkylation (cracking) and dehydrogenation. Cracking of cumene is generally attributed to the action of Brønsted sites by a carbonium ion mechanism while dehydrogenation of cumene yields α -methylstyrene as the major product, the formation of which has been ascribed to the Lewis acid sites.^{46–48} The selectivity towards dehydrogenated products may thus be related to the Lewis acidity of the systems and the generation of cracking products with the Brønsted acidity of the systems.

Considerable enhancement of weak, medium and strong acid sites is observed in the NH₃-TPD profile after the incorporation of sulphate species on the pure SnO₂ and V₂O₅-supported systems. We noted a regular increase in different acid sites in the unmodified V₂O₅/SnO₂ samples with increase in V₂O₅ content (results not given here). However this was not observed in the case of the sulphated series. The strength of medium acid sites increased up to 9 mass % V₂O₅ loading and then declined for higher V₂O₅ loadings, while the weak and strong acid site concentrations reached a maximum at 6 mass % V₂O₅. The selectivity towards the hydrocracking also showed a marginal increase with sulphate loading up to 9 mass % V₂O₅, which dropped off thereafter at high vanadia loadings. This pattern is in harmony with the amount of medium acid sites measured by NH₃-TPD.

The initial enhancement of acidity can be attributed to the increase of the electron-accepting properties of the three coordinated metal cations *via* the inductive effect of sulphate anions, which withdraw electron density through the bridging oxygen atom.^{49,50} According to the dual Brønsted-Lewis site model proposed by Clearfield,⁵¹ uncalcined catalyst contains protons as bisulphate and as hydroxyl groups bridging two metal ions. During calcination, either the bisulphate anion can react with an adjacent hydroxyl group, resulting in a Lewis acid site, or two adjacent hydroxyl groups can interact keeping the bisulphate ion intact, thereby generating Brønsted acidity. The combination of these Brønsted sites with the adjacent Lewis sites can also generate strong acidity. The number and strength of all types of

acid sites are increased again by gradually escalating the vanadium oxide content. The steady increase in the acidity values with vanadia content has already been reported in the case of supported metal oxides.^{52,53} However, the drastic reduction in the acidity values for high vanadia-containing sulphated systems may be due to the higher amount of sulphate retained on the surface. Elemental analysis by EDX also revealed that the amount of sulphate retained is higher for systems with high vanadium oxide content (Table 1). The decrease in surface acidity at high concentration of sulphate is probably due to the formation of polysulphate, which reduces the number of Brønsted sites and consequently that of the total acid sites.⁵⁴

The catalytic efficiency of sulphated V₂O₅/SnO₂ catalysts was tested for vapour phase Beckmann rearrangement (Table 2). The results showed that the sulphated systems are much superior to pure tin oxide in their activity. The V₂O₅-containing samples gave more than 90% cyclohexanone oxime conversion and the maximum activity was shown by ST9, where the conversion reached 100%. We also noted that the conversion pattern is in concurrence with the Brønsted acidity calculated from the cumene cracking reaction and the concentration of medium acid sites from NH₃-TPD. Hence it is clear that the Brønsted acid sites are responsible for the formation of ϵ -caprolactam sulphated V₂O₅/SnO₂ catalysts. There is a definite correlation between the amount of ammonia desorbed from the medium acid sites and the catalytic efficiency. The agreement between the conversion rates with the surface area of the catalyst shows that the surface properties also play an important role in the surface activity of the catalysts. Scrutiny of the selectivity pattern with the acidity data (Table 2) suggests that the ϵ -caprolactam selectivity depends strongly on the medium acid site and the Brønsted acidity structure of the prepared catalysts.

Curtin *et al.*⁵⁵ investigated the effect of concentration of intermediate acid sites from ammonia-TPD measurements on the activity and selectivity of the Beckmann rearrangement using B₂O₃/Al₂O₃ catalysts. They reported that B₂O₃/Al₂O₃ catalysts with the largest concentration of intermediate strength acid sites exhibited excellent selectivity for ϵ -caprolactam. Ushikubo *et al.*⁴ reported for the H-ZSM-5 zeolite modified by B₂O₃ that lactam selectivity improved with an increase of the ratio of weak acid sites to strong acid sites.⁵⁶ It has been reported that a relatively strong acid site ($H_0 < -5.6$) of B₂O₃/SiO₂ is responsible for the formation of ϵ -caprolactam.⁵⁷ Mao *et al.*^{58,59} also proposed that the order of ϵ -caprolactam selectivity is dependent on the percentage of medium strength acid sites.

The good agreement between the surface properties and the Brønsted acidity values (obtained from cracking product selec-

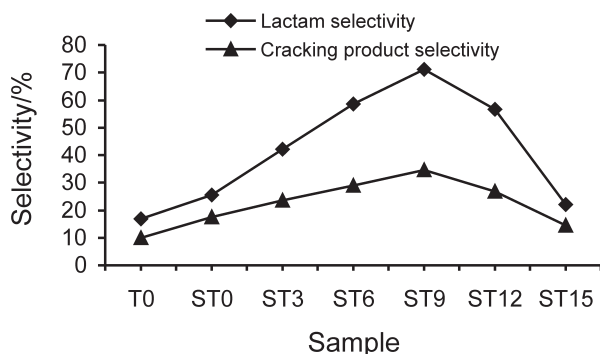


Figure 5 Correlation of Brønsted acidity (cracking product selectivity) with ϵ -caprolactam selectivity in the vapour phase Beckmann rearrangement.

tivity in the cumene conversion reaction) and the cyclohexanone conversion lactam selectivity data as presented in Fig. 5 suggests that all the Brønsted acid sites are the active sites in the rearrangement reaction. The lactam selectivity results are also in agreement with the medium acid strength of the samples obtained from the ammonia-TPD method (see Table 2). The results are in line with earlier reports in which the active sites for cyclohexanone oxime conversion in the Beckmann rearrangement were reported as intermediate strength acid sites. The dependence of selectivity on the surface properties implies that there are some factors, other than the surface concentration of acid sites, which also play a crucial role in determining the catalytic activity. The diffusion rate of ϵ -caprolactam could depend on the pore structure and the fine pores seem to fill the effective role of diffusion.³

Figure 6 presents the time course of the Beckmann rearrangement over ST6, where cyclohexanone oxime conversion and the selectivity pattern obtained for ϵ -caprolactam and cyclohexanone are plotted as functions of reaction time. From Fig. 6, it is seen that the activity of ST6 declines continuously with reaction time from 100% to about 50% after 5 h on stream. The observations on the catalyst deactivation are consistent with the possibility of neutralization of active acid sites by the basic reactants and products formed.¹² Although the oxime conversion decreases with reaction time, no significant change in lactam selectivity is observed. The selectivity to ϵ -caprolactam changes during the first 2 h and remains constant at 81% thereafter. The selectivity to cyclohexanone also remains almost constant for the 5 h on-stream experiment, in spite of the declining oxime conversion.

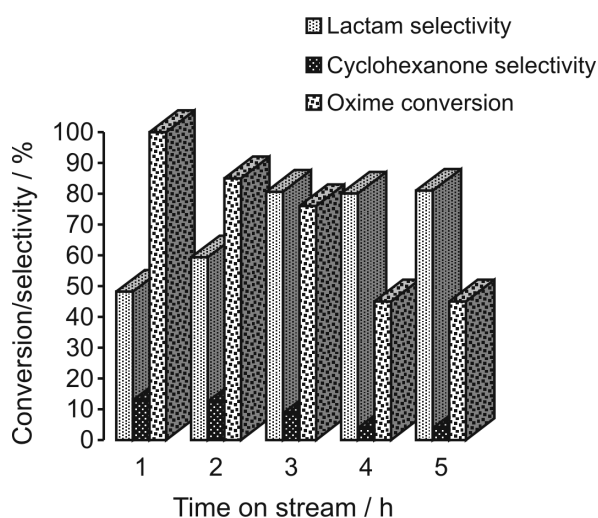


Figure 6 Effect of time-on-stream on catalyst activity and selectivity (ST6, sulphate-modified T6).

4. Conclusions

We demonstrate that sulphate-modified V_2O_5/SnO_2 solid acid catalysts with large surface area can be prepared by a simple impregnation method. Synthesis of ϵ -caprolactam in quantitative yields is one of the potential applications of these eco-friendly catalysts. The active sites for vapour phase Beckmann rearrangement are found to be the medium strength acid sites on the catalyst surface. The vanadia and sulphate content on the catalyst surface are observed to affect the surface properties and hence the catalyst activity and selectivity. Sulphated V_2O_5/SnO_2 with 9 mass % vanadia loading exhibits excellent performance among the investigated catalysts for the Beckmann rearrangement. Time-on-stream studies revealed that the oxime conversion declined significantly while the lactam and cyclohexanone selectivity remained steady during a 5 h reaction run.

References

- J.E. Kent and S. Riegel, *Handbook of Industrial Chemistry*, 8th edn., Van Nostrand, New York, USA, 1983, p. 402.
- D.S. Mao, G.Z. Lu and Q.L. Chen, *Appl. Catal. A. Gen.*, 2005, **279**, 145–153.
- O. Immel, H.H. Schwarz, K. Starke and W. Swodenk, *Chem. Ing. Tech.*, 1984, **56**, 612–613.
- T. Ushikubo and K. Wada, *J. Catal.*, 1994, **148**, 138–148.
- D. Shouro, Y. Ohya, S. Mishima and T. Nakajima, *Appl. Catal. A. Gen.*, 2001, **214**, 59–67.
- K. Chaudhari, R. Bal, A. Chandwadkar and S. Sivasanker, *J. Mol. Catal. A. Chem.*, 2002, **177**, 247–253.
- L. Forni, C. Tosi, G. Fornassari, F. Trifiro, A. Vaccari and J.B. Nagy, *J. Mol. Catal. A. Chem.*, 2004, **221**, 97–103.
- G.P. Heitmann, G. Dahlhoff, J.P.M. Niederer and W.F. Hölderich, *J. Catal.*, 2000, **194**, 122–129.
- J.-C. Chang and A.-N. Ko, *Catal. Today*, 2004, **97**, 241–247.
- T. Komatsu, T. Maeda and T. Yashima, *Micropor. Mesopor. Mater.*, 2000, **35–36**, 173–180.
- A. Aucejo, M.C. Burguet, A. Corma and V. Fornes, *Appl. Catal.*, 1986, **22**, 187–200.
- H. Ichihashi, M. Ishida, A. Shiga, M. Kitamura, T. Suzuki, K. Suenobu and K. Sugita, *Catal. Survey Asia*, 2003, **7**, 261–270.
- M. Ghiaci, A. Abbaspur and R.J. Kalbasi, *Appl. Catal. A. Gen.*, 2005, **287**, 83–88.
- D.S. Mao, G.Z. Lu, Q.L. Chen, Z.K. Xie and Y.X. Zhang, *Catal. Lett.*, 2001, **77**, 119–124.
- D.S. Mao, Q.L. Chen and G.Z. Lu, *React. Kinet. Catal. Lett.*, 2002, **75**, 75–80.
- D.S. Mao, G.Z. Lu and Q.L. Chen, *Appl. Catal. A. Gen.*, 2005, **244**, 145–153.
- X. Guo, W. Hou, W. Ding, Y. Fan, Q. Yan and Y. Chen, *Micropor. Mesopor. Mater.*, 2005, **80**, 269–274.
- K. Arata, *Appl. Catal.*, 1996, **146**, 3–32.
- J.G. Eon, R. Olier and J.-C. Volta, *J. Catal.*, 1994, **145**, 318–326.
- H.H. Kung and M.C. Kung, *Appl. Catal. A*, 1997, **157**, 105–116.
- A. Khodakov, B. Olthof, A.T. Bell and E. Iglesia, *J. Catal.*, 1999, **181**, 205–216.
- I.E. Wachs, R.Y. Saleh, S.S. Chan and C.C. Chersch, *Appl. Catal. A*, 1985, **15**, 339.
- H. Bosch and F. Janssen, *Catal. Today*, 1988, **15**, 339–352.
- B.M. Reddy, A. Khan, Y. Yamada, T. Kobayashi, S. Loidant and J.-C. Volta, *J. Phys. Chem. B*, 2002, **106**, 10964–10972.
- J. Matta, D. Courcot, E.A. Aad and A. Aboukais, *Chem. Mater.*, 2002, **14**, 4118–4125.
- J. Buiten, *J. Catal.*, 1968, **10**, 188–199.
- M. Ai and S. Suzuki, *Shokubai*, 1973, **15**, 159.
- T. Seiyama, M. Egashira, T. Sakamoto and I. Aso, *J. Catal.*, 1972, **24**, 76–81.
- J.R. Sohn, S.G. Cho, Y.I. Pae and S. Hayashi, *J. Catal.*, 1996, **150**, 170–177.

- 30 H. Matsuhashi, M. Hino and K. Arata, *Appl. Catal.*, 1990, **59**, 205–212.
- 31 A. Corma, *Chem. Rev.*, 1995, **95**, 559–614.
- 32 X. Song and A. Sayari, *Catal. Rev. Sci. Eng.*, 1996, **38**, 329–412.
- 33 A.K. Dalai, R. Sethuraman, S.P.R. Katikeni and R.O. Idem, *Ind. Eng. Chem. Res.*, 1998, **37**, 3869–3878.
- 34 S.K. Samantray, T. Mishra and K.M. Parida, *J. Mol. Catal. A. Gen.*, 2000, **156**, 267–274.
- 35 K. Hadjiivanov, A. Davydov and D. Klissurski, *Kinet. Catal.*, 1988, **29**, 161–167.
- 36 I. E. Wachs, *Catal. Today*, 1996, **27**, 437–455.
- 37 G. Busca, G. Centi, L. Marchetti and F. Trifiro, *Langmuir*, 1989, **2**, 568–576.
- 38 N.Y. Topsoe, H. Topsoe and J.A. Dumesic, *J. Catal.*, 1995, **151**, 226–240.
- 39 C. Morterra, G. Cerrato, C. Emanuel and V. Bolis, *J. Catal.*, 1993, **142**, 349–367.
- 40 M. Pontzi, C. Duschatzky, A. Carraseull and E. Ponzi, *Appl. Catal. A. Gen.*, 1998, **169**, 373–379.
- 41 R. Srinivasan, R.A. Keogh, D.R. Milburn and B.H. Davis, *J. Catal.*, 1995, **153**, 123–130.
- 42 H. Eckert, G. Deo, I. E. Wachs and A. M. Hirt, *Coll. Surf.*, 1995, **45**, 347–359.
- 43 G. Deo and I.E. Wachs, *J. Phys. Chem.*, 1991, **95**, 5889–5895.
- 44 F. Roozeboom, M.C. Mittemeijer, J.A. Moulijn, J. Medema, V.H. J. de Beer and P.J. Gellings, *J. Phys. Chem.*, 1980, **84**, 2783–2791.
- 45 A. Francesco, D. Roberto and P. Adolfo, *Appl. Catal. A. Gen.*, 1998, **170**, 127–137.
- 46 H.G. Karge and V. Dondur, *J. Phys. Chem.*, 1990, **94**, 765–772.
- 47 A. Corma and B.W. Wojciechowski, *Catal. Rev. Sci. Eng.*, 1982, **24**, 1–65.
- 48 W. Przystajko, R. Fiedorow and I.G. Dalla Lana, *Appl. Catal.*, 1985, **15**, 265–272.
- 49 T. Yamaguchi, *Appl. Catal.*, 1990, **61**, 1–25.
- 50 A. Corma, V. Fornes, M.I. Juan Rajadell and J.M. Lopez Nieto, *Appl. Catal. A. Gen.*, 1994, **116**, 151–158.
- 51 A. Clearfield, G.P.D. Serrete and A.H. Khazi-Syed, *Catal. Today*, 1994, **20**, 295–312.
- 52 M. Ai, *J. Catal.*, 1975, **40**, 318–326.
- 53 M. Ai, *Bull. Chem. Soc. Jpn.*, 1976, **49**, 1328–1334.
- 54 A. K. Dalai, R. Sethuraman, S.P.R. Katikeni and R.O. Idem, *Ind. Eng. Chem. Res.*, 1998, **37**, 3869–3878.
- 55 T. Curtin, J.B. McMonagle, M. Ruwett and B.K. Hodnett, *J. Catal.*, 1993, **142**, 172–181.
- 56 BASE Ger. Patent, No. 1, 1967, 227 028.
- 57 B.-Q. Xu, S.-B. Cheng, S. Jiang and Q.-M. Zhu, *Appl. Catal. A. Gen.*, 1999, **188**, 361–368.
- 58 D.S. Mao, Q.L. Chen and G.Z. Lu, *Appl. Catal. A. Gen.*, 2003, **244**, 273–282.
- 59 D.S. Mao, G.Z. Lu and Q.L. Chen, *Appl. Catal. A. Gen.*, 2005, **279**, 145–153.